

PACS numbers: 42.50.Gy; 42.50.Hz; 42.50.–p
DOI: 10.1070/QE2015v045n01ABEH015508

Phase-dependent high refractive index without absorption in a four-level inverted-Y atomic system

Zhi-Qiang Zeng, Yu-Ping Wang, Fu-Ti Liu, Zeng-Hui Gao

Abstract. **We consider a closed four-level inverted-Y system in the presence and the absence of a microwave field. It is found that due to the quantum coherence between the two lower levels, either induced by the spontaneous decay or by the microwave field, the refraction–absorption properties of the system can be modulated by controlling the relative phase of the applied fields in both driven ways. In particular, by properly setting the values of the relative phase, the desirable high index of refraction without absorption can be achieved.**

Keywords: *quantum coherence, high refractive index without absorption, relative phase.*

1. Introduction

Recent years have seen considerable interest in optical control over the refractive index properties of a medium [1–5]. As is known, the absorption of the light is large at the detuning at which the resonant index of refraction is large. For example, the large refractive index of a medium consisting of two-level atoms means that such a medium exhibits considerable optical absorption. But it should be pointed out that the refractive index properties can be modified by the quantum coherence in multi-level atomic systems. As a result of the quantum coherence, the system exhibits little absorption with a high refractive index in a three-level atom [6–11]. The enhancement of the index of refraction has been evidenced in various experiments [12–14]. In an optically dense medium, it can be expected that a closed excitation contour will result in quasi-periodic variations of the refractive index [15]. Recently, we have investigated the effect of the relative phase on the refraction–absorption properties in a closed interaction contour formed by applying a microwave field between the excited levels of the system [16, 17]. Inspired by these studies we discuss in this paper the phase-dependent refraction–absorption properties, which is of interest for using in quantum memory systems [5, 18] and designing inversionless lasers [19, 20].

In this paper, we study a closed four-level inverted-Y system with or without a microwave field, which can be experimentally realised in rubidium atoms [21, 22]. Such an atomic configuration has received much attention. Yan et al. [21] observed the suppression of two-photon absorption in a cold ^{87}Rb atom. The study of the Autler–Townes effect was experimentally demonstrated in a sodium dimer by Ahmed et al. [23]. Subsequently the coherent optical detection of highly excited Rydberg states was implemented by Mohapatra et al. [24]. Recently, Tian et al. [25] reported an experimental observation of the effect of quantum coherence on absorption in a rubidium atomic beam. At the same time, it was theoretically shown that such an inverted-Y system can exhibit many interesting phenomena, such as double electromagnetically induced transparency [26, 27], spontaneous emission quenching [28], cross-Kerr nonlinearity [29] and coherent population transfer [30]. Many these studies were related to the quantum coherence, but the influence of the relative phase of the applied fields on the refraction–absorption properties was not examined. In the present work, we demonstrate the effect of the relative phase on the refraction–absorption properties in an inverted-Y system, and find that a high index of refraction without absorption can be always achieved by controlling the relative phase.

2. Phenomena due to spontaneously generated coherence in an inverted-Y system

The system of a closed four-level inverted-Y atom is shown in Fig. 1a. A weak probe field $\mathcal{E}_1$ at frequency ω_1 and a coupling field $\mathcal{E}_3$ at frequency ω_3 with corresponding Rabi frequencies $G_1 = \mu_{21}\mathcal{E}_1/\hbar$ and $G_3 = \mu_{24}\mathcal{E}_3/\hbar$ are applied to the atomic transitions $|2\rangle \leftrightarrow |1\rangle$ and $|2\rangle \leftrightarrow |4\rangle$, respectively. A pump field $\mathcal{E}_2$ at frequency ω_2 is applied to the atomic transition $|3\rangle \leftrightarrow |2\rangle$ with a Rabi frequency $G_2 = \mu_{32}\mathcal{E}_2/\hbar$. We assume throughout the paper that the Rabi frequency G_2 is a real parameter. Incoherent pumping with a rate 2Λ interacts with the transition $|1\rangle \leftrightarrow |2\rangle$ to prepare a small quantity of atoms in the excited level $|2\rangle$. The spontaneous decay rates from $|3\rangle$ to $|2\rangle$, $|2\rangle$ to $|4\rangle$ and $|2\rangle$ to $|1\rangle$ are equal to $2\gamma_2$, $2\gamma_3$ and $2\gamma_1$, respectively.

The Hamiltonian under the dipole and rotation-wave approximation is given by

$$\hat{H}_I = -\hbar\Delta_1|1\rangle\langle 1| + \hbar\Delta_2|3\rangle\langle 3| - \hbar\Delta_3|4\rangle\langle 4|$$

$$-\hbar(G_1|2\rangle\langle 1| + G_2|3\rangle\langle 2| + G_3|2\rangle\langle 4| + \text{H.c.}, \qquad (1)$$

Zhi-Qiang Zeng College of Physics and Electronic Engineering, Yibin University, Yibin 644000, P.R. China; Computational Physics Key Laboratory of Sichuan Province, Yibin University, Yibin 644000, P.R. China; e-mail: zhiqiang_zeng@163.com;
Yu-Ping Wang College of Mining and Safety Engineering, Yibin University, Yibin 644000, P.R. China;
Fu-Ti Liu College of Physics and Electronic Engineering, Yibin University, Yibin 644000, P.R. China;
Zeng-Hui Gao Computational Physics Key Laboratory of Sichuan Province, Yibin University, Yibin 644000, P.R. China

Received 4 April 2014; revision received 7 August 2014
Kvantovaya Elektronika **45** (1) 41–46 (2015)
Submitted in English

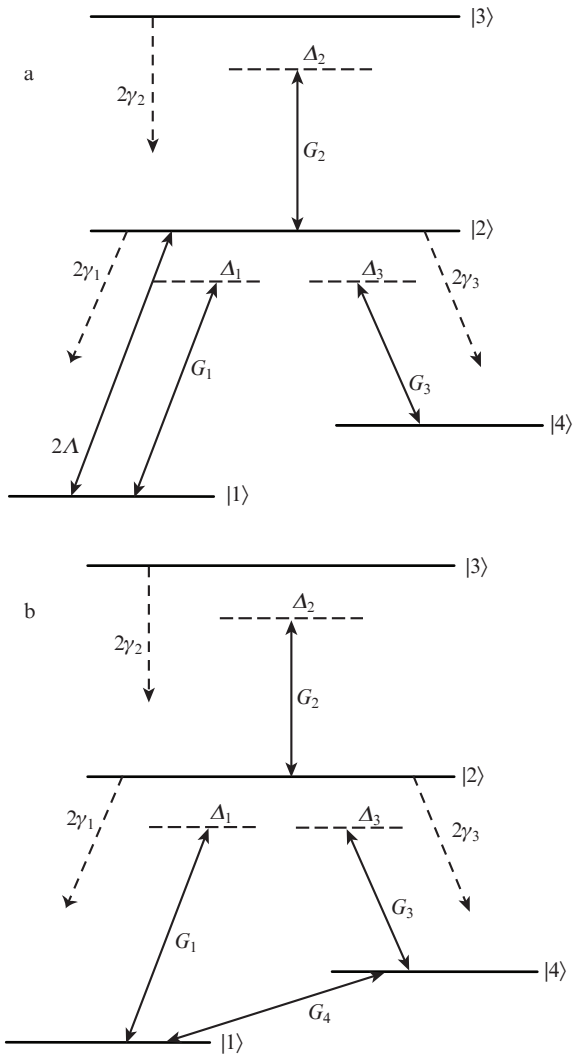

Figure 1. Energy scheme under consideration: (a) a four-level inverted-Y atom with the electric dipole forbidden transition between levels $|4\rangle$ and $|1\rangle$ and (b) the same atom driven by a microwave field on the transition $|4\rangle \leftrightarrow |1\rangle$ through an allowed magnetic dipole transition.

where the detunings of the probe, pump and coupling laser radiations are given by $\Delta_1 = \omega_{21} - \omega_1$, $\Delta_2 = \omega_{32} - \omega_2$ and $\Delta_3 = \omega_{24} - \omega_3$, respectively. The dynamic evolution of the system is governed by the master equation of the density matrix

$$\frac{\partial\hat{\sigma}}{\partial t} = -\frac{\mathrm{i}}{\hbar}[\hat{H}_I,\hat{\sigma}] - (\gamma_1+\gamma_3+\Lambda)\{|2\rangle\langle 2|,\hat{\sigma}\}$$
$$-\gamma_2\{|3\rangle\langle 3|,\hat{\sigma}\} - \Lambda\{|1\rangle\langle 1|,\hat{\sigma}\} + (2\gamma_1+2\Lambda)|1\rangle\langle 2|\hat{\sigma}|2\rangle\langle 1|$$
$$+ 2\gamma_2|2\rangle\langle 3|\hat{\sigma}|3\rangle\langle 2| + 2\gamma_3|4\rangle\langle 2|\hat{\sigma}|2\rangle\langle 4| + 2\Lambda|2\rangle\langle 1|\hat{\sigma}|1\rangle\langle 2|$$
$$+\eta(|1\rangle\langle 2|\hat{\sigma}|2\rangle\langle 4| + |4\rangle\langle 2|\hat{\sigma}|2\rangle\langle 1|), \qquad (2)$$

where the square and curly brackets denote the commutation and anticommutation of therein operators, respectively. The non-zero parameter $\eta = 2\sqrt{\gamma_1\gamma_3}\cos\theta$ (θ is the angle between the dipole matrix elements $\boldsymbol{\mu}_{21}$ and $\boldsymbol{\mu}_{24}$) represents the quantum coherence effect resulted from the cross-coupling between two decay paths $|2\rangle \to |1\rangle$ and $|2\rangle \to |4\rangle$, i.e., the spontaneously generated coherence (SGC) effect. Due to the existence of the SGC effect, this system can be related to the relative phase between the probe and coupling fields. Thus, we treat the Rabi frequencies G_1 and G_3 as complex parameters: $G_1 = \Omega_1\exp(\mathrm{i}\phi_1)$ and $G_3 = \Omega_3\exp(\mathrm{i}\phi_3)$, where ϕ_1 and ϕ_3 are the phases of the probe and coupling fields, respectively. Let $G_2 = \Omega_2$, $\sigma_{ii} = \rho_{ii}$, $\sigma_{23} = \rho_{23}$, $\sigma_{12} = \rho_{12}\exp(-\mathrm{i}\phi_1)$, $\sigma_{13} = \rho_{13} \times \exp(-\mathrm{i}\phi_1)$, $\sigma_{42} = \rho_{42}\exp(-\mathrm{i}\phi_3)$, $\sigma_{43} = \rho_{43}\exp(-\mathrm{i}\phi_3)$ and $\sigma_{14} = \rho_{14}\exp(\mathrm{i}\Phi)$, where $\Phi = \phi_3 - \phi_1$ is the relative phase of the applied fields. Then, the redefined matrix elements ρ_{ij} ($i,j = 1,2,3,4$) obey the differential equations as follows:

$$\dot{\rho}_{11} = -2\Lambda\rho_{11} + 2(\gamma_1+\Lambda)\rho_{22} - \mathrm{i}\Omega_1\rho_{12} + \mathrm{i}\Omega_1\rho_{21},$$
$$\dot{\rho}_{33} = -2\gamma_2\rho_{33} + \mathrm{i}\Omega_2\rho_{23} - \mathrm{i}\Omega_2\rho_{32},$$
$$\dot{\rho}_{44} = 2\gamma_3\rho_{22} - \mathrm{i}\Omega_3\rho_{42} + \mathrm{i}\Omega_3\rho_{24},$$
$$\dot{\rho}_{21} = -(\gamma_1+\gamma_3+2\Lambda+\mathrm{i}\Delta_1)\rho_{21}$$
$$+\mathrm{i}\Omega_1(\rho_{11}-\rho_{22}) + \mathrm{i}\Omega_2\rho_{31} + \mathrm{i}\Omega_3\rho_{41},$$
$$\dot{\rho}_{31} = -(\gamma_2+\Lambda+\mathrm{i}\Delta_1+\mathrm{i}\Delta_2)\rho_{31} + \mathrm{i}\Omega_2\rho_{21} - \mathrm{i}\Omega_1\rho_{32},$$
$$\dot{\rho}_{32} = -(\gamma_1+\gamma_2+\gamma_3+\Lambda+\mathrm{i}\Delta_2)\rho_{32} \qquad (3)$$
$$+\mathrm{i}\Omega_2(\rho_{22}-\rho_{33}) - \mathrm{i}\Omega_1\rho_{31} - \mathrm{i}\Omega_3\rho_{34},$$
$$\dot{\rho}_{41} = -(\Lambda+\mathrm{i}\Delta_1-\mathrm{i}\Delta_3)\rho_{41} + \mathrm{i}\Omega_3\rho_{21}$$
$$-\mathrm{i}\Omega_1\rho_{42} + \eta\rho_{22}\exp(\mathrm{i}\Phi),$$
$$\dot{\rho}_{42} = -(\gamma_1+\gamma_3+\Lambda-\mathrm{i}\Delta_3)\rho_{42}$$
$$+\mathrm{i}\Omega_3(\rho_{22}-\rho_{44}) - \mathrm{i}\Omega_1\rho_{41} - \mathrm{i}\Omega_2\rho_{43},$$
$$\dot{\rho}_{43} = -(\gamma_2-\mathrm{i}\Delta_2-\mathrm{i}\Delta_3)\rho_{43} + \mathrm{i}\Omega_3\rho_{23} - \mathrm{i}\Omega_2\rho_{42}.$$

The above density matrix elements additionally obey the normalisation and Hermitian condition:

$$\sum_{i=1}^{4}\rho_{ii} = 1 \text{ and } \rho_{ij} = \rho_{ji}^{*}.$$

It is obvious from Eqn (3) that the term including the relative phase Φ will disappear if the SGC effect is absent. Here the properties of this scheme depend on the relative phase in the presence of the SGC effect. As is known, the refractive index and absorption for the probe field correspond to the real and imaginary parts of polarisation ρ_{21}, respectively. We assume for simplicity that values of the parameters Ω_1, Ω_2, Ω_3, Λ, Δ_1, Δ_2, Δ_3, γ_2 and γ_3 are normalised to γ_1.

Now, let us investigate the refraction–absorption relation of the weak probe field for the steady state. In the system under study, the strong resonant coupling field dresses the states $|2\rangle$ and $|4\rangle$. The dressed states can be written as

$$|+\rangle = \frac{1}{\sqrt{2}}(|2\rangle + |4\rangle) \text{ and } \quad |-\rangle = \frac{1}{\sqrt{2}}(|2\rangle - |4\rangle).$$

The eigenvalues of the two dressed states are Ω_3 and $-\Omega_3$.

Figure 2 shows the dependences of the refractive index and the absorption coefficient on the probe detuning Δ_1. One can see that for the relative phase Φ under study, a high index of refraction can always correspond to zero absorption (points A, B and C in Figs 2a, 2b and 2c, respectively). But

these points are clearly located at different detunings for different values of Φ. In Fig. 2a ($\Phi = 3\pi/2$), the high index of refraction without absorption is located at $\Delta_1 = 0$; in Fig. 2b ($\Phi = 0$), – at $\Delta_1 = \Omega_3$, which corresponds to first eigenvalue of the two dressed states; and in Fig. 2c ($\Phi = \pi$), – at $\Delta_1 = -\Omega_3$, which corresponds to the second eigenvalue of the two dressed states.

To gain a deeper insight into the dependence of the refraction–absorption relation on the relative phase Φ, we performed additional numerical calculations and found that the maximum index of refraction always corresponds to zero absorption at the appropriate values of the relative phase Φ. With different probe field detunings, the high index of refraction without absorption can be always achieved by choosing the proper values of Φ. As an example, Fig. 3 shows the dependences of $\mathrm{Re}\rho_{21}$ and $\mathrm{Im}\rho_{21}$ on the relative phase Φ for several different values of the probe detunings: $\Delta_1 = 0$ and $\pm\Omega_3$. It can be shown that the high indices of refraction without absorption are achieved periodically in the relative phase Φ. For $\Delta_1 = 0$ (Fig. 3a), it can be achieved at $\Phi = 2k\pi + 3\pi/2$ ($k = 0, \pm 1, \pm 2 \ldots$; points A_1, A_2); for $\Delta_1 = \Omega_3$ (Fig. 3b), – at $\Phi = 2k\pi$ (points B_1, B_2, B_3); and for $\Delta_1 = -\Omega_3$ (Fig. 3c), – at $\Phi = 2k\pi + \pi$ (points C_1, C_2).

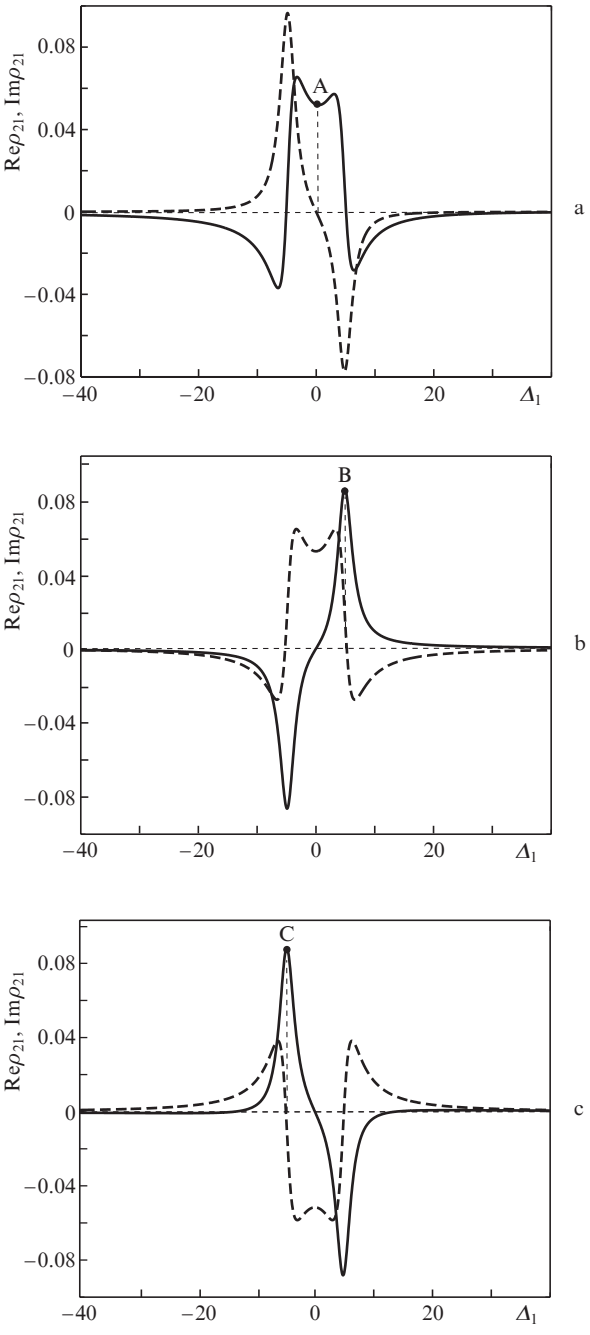

Figure 2. $\mathrm{Re}\rho_{21}$ (solid curves) and $\mathrm{Im}\rho_{21}$ (dashed curves) vs. probe detuning Δ_1 at Φ = (a) $3\pi/2$, (b) 0 and (c) π ($\gamma_1 = \gamma_2 = \gamma_3 = 1$, $\theta = \pi/6$, $\Omega_1 = 0.1\sin\theta$, $\Omega_2 = 0.5$, $\Omega_3 = 10\sin\theta$, $\Delta_2 = -\Delta_1$, $\Delta_3 = 0$, $\Lambda = 0.3$).

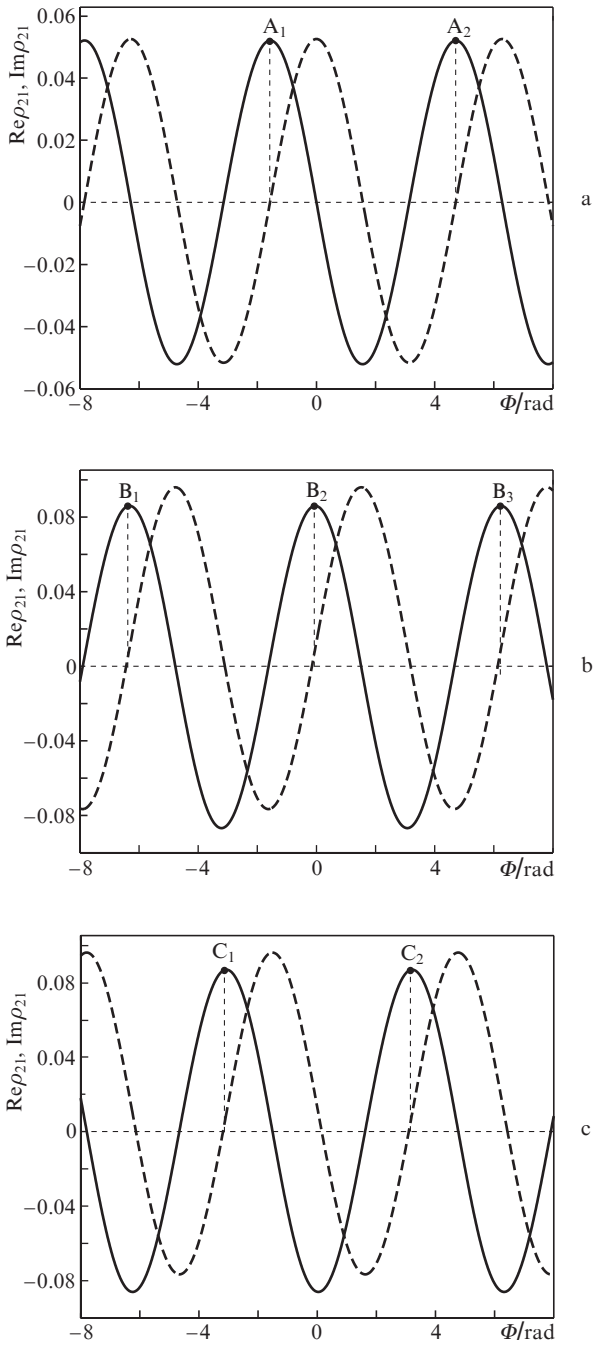

Figure 3. $\mathrm{Re}\rho_{21}$ (solid curves) and $\mathrm{Im}\rho_{21}$ (dashed curves) vs. relative phase Φ at probe detuning Δ_1 = (a) 0, (b) Ω_3 and (c) $-\Omega_3$. Other parameters are the same as those in Fig. 2.

3. Phenomena due to microwave-induced coherence in an inverted-Y system

In Fig. 1b, a resonant microwave field with the Rabi frequency G_4 is coupled to the transition $|4\rangle \leftrightarrow |1\rangle$ through an allowed magnetic transition. In this scheme, the quantum coherence is achieved by coupling the two lower levels of the inverted-Y system by means of the microwave field; therefore, we refer to it as microwave-induced coherence [16, 17]. Since orthogonal dipoles for two transitions with small energy separation are more easily found in nature, we assume the dipole matrix elements (i.e., $\boldsymbol{\mu}_{21}$ and $\boldsymbol{\mu}_{24}$) to be orthogonal thereby excluding the SGC effect, which is more convenient in its experimental realisation.

In this case, the Hamiltonian under the dipole and rotation–wave approximation is given by

$$\hat{H}_I = -\hbar\Delta_1|1\rangle\langle 1| + \hbar\Delta_2|3\rangle\langle 3| - \hbar\Delta_3|4\rangle\langle 4|$$

$$-\hbar(G_1|2\rangle\langle 1| + G_2|3\rangle\langle 2| + G_3|2\rangle\langle 4| + G_4|4\rangle\langle 1| + \text{H.c.} \qquad (4)$$

The dynamic evolution of the system is governed by the master equation of the density matrix

$$\frac{\partial\hat{\sigma}}{\partial t} = -\frac{\mathrm{i}}{\hbar}[\hat{H}_I,\hat{\sigma}] - (\gamma_1+\gamma_3)\{|2\rangle\langle 2|,\hat{\sigma}\} - \gamma_2\{|3\rangle\langle 3|,\hat{\sigma}\}$$

$$+ 2\gamma_1|1\rangle\langle 2|\hat{\sigma}|2\rangle\langle 1| + 2\gamma_2|2\rangle\langle 3|\hat{\sigma}|3\rangle\langle 2| + 2\gamma_3|4\rangle\langle 2|\hat{\sigma}|2\rangle\langle 4|. \qquad (5)$$

As the system is sensitive to the phases of the probe, coupling and microwave fields because of the characteristic of the 'closed-loop' configuration constructed by the levels $|1\rangle$, $|2\rangle$ and $|4\rangle$ with their driving fields, we treat the Rabi frequencies G_1, G_3 and G_4 as complex parameters: $G_1 = \Omega_1\exp(\mathrm{i}\phi_1)$, $G_3 = \Omega_3 \times \exp(\mathrm{i}\phi_3)$ and $G_4 = \Omega_4\exp(\mathrm{i}\phi_4)$, where ϕ_1, ϕ_3 and ϕ_4 are the phases of the probe, coupling and microwave fields, respectively. Let $G_2 = \Omega_2$, $\sigma_{ii} = \rho_{ii}$, $\sigma_{23} = \rho_{23}$, $\sigma_{12} = \rho_{12}\exp(-\mathrm{i}\phi_1)$, $\sigma_{13} = \rho_{13}\exp(-\mathrm{i}\phi_1)$, $\sigma_{42} = \rho_{42}\exp(-\mathrm{i}\phi_3)$, $\sigma_{43} = \rho_{43}\exp(-\mathrm{i}\phi_3)$ and $\sigma_{14} = \rho_{14}\exp(\mathrm{i}\phi_3 - \mathrm{i}\phi_1)$. Then the redefined matrix elements ρ_{ij} $(i,j = 1, 2, 3, 4)$ obey the differential equations as follows:

$$\dot{\rho}_{11} = 2\gamma_1\rho_{22} - \mathrm{i}\Omega_1\rho_{12} + \mathrm{i}\Omega_1\rho_{21} - \mathrm{i}\Omega_4\rho_{14}\exp(\mathrm{i}\Phi) + \mathrm{i}\Omega_4\rho_{41}\exp(-\mathrm{i}\Phi),$$

$$\dot{\rho}_{33} = -2\gamma_2\rho_{33} + \mathrm{i}\Omega_2\rho_{23} - \mathrm{i}\Omega_2\rho_{32},$$

$$\dot{\rho}_{44} = 2\gamma_3\rho_{22} - \mathrm{i}\Omega_3\rho_{42} + \mathrm{i}\Omega_3\rho_{24} + \mathrm{i}\Omega_4\rho_{14}\exp(\mathrm{i}\Phi) - \mathrm{i}\Omega_4\rho_{41}\exp(-\mathrm{i}\Phi),$$

$$\dot{\rho}_{21} = -(\gamma_1+\gamma_3+\mathrm{i}\Delta_1)\rho_{21} + \mathrm{i}\Omega_1(\rho_{11}-\rho_{22}) + \mathrm{i}\Omega_2\rho_{31} + \mathrm{i}\Omega_3\rho_{41} - \mathrm{i}\Omega_4\rho_{24}\exp(\mathrm{i}\Phi),$$

$$\dot{\rho}_{31} = -(\gamma_2+\mathrm{i}\Delta_1+\mathrm{i}\Delta_2)\rho_{31} + \mathrm{i}\Omega_2\rho_{21} - \mathrm{i}\Omega_1\rho_{32} - \mathrm{i}\Omega_4\rho_{34}\exp(\mathrm{i}\Phi), \qquad (6)$$

$$\dot{\rho}_{32} = -(\gamma_1+\gamma_2+\gamma_3+\mathrm{i}\Delta_2)\rho_{32} + \mathrm{i}\Omega_2(\rho_{22}-\rho_{33}) - \mathrm{i}\Omega_1\rho_{31} - \mathrm{i}\Omega_3\rho_{34},$$

$$\dot{\rho}_{41} = -(\mathrm{i}\Delta_1 - \mathrm{i}\Delta_3)\rho_{41} + \mathrm{i}\Omega_3\rho_{21} - \mathrm{i}\Omega_1\rho_{42} + \mathrm{i}\Omega_4(\rho_{11}-\rho_{44})\exp(\mathrm{i}\Phi),$$

$$\dot{\rho}_{42} = -(\gamma_1+\gamma_3-\mathrm{i}\Delta_3)\rho_{42} + \mathrm{i}\Omega_3(\rho_{22}-\rho_{44}) - \mathrm{i}\Omega_1\rho_{41} - \mathrm{i}\Omega_2\rho_{43} + \mathrm{i}\Omega_4\rho_{12}\exp(\mathrm{i}\Phi),$$

$$\dot{\rho}_{43} = -(\gamma_2 - \mathrm{i}\Delta_2 - \mathrm{i}\Delta_3)\rho_{43} + \mathrm{i}\Omega_3\rho_{23} - \mathrm{i}\Omega_2\rho_{42} + \mathrm{i}\Omega_4\rho_{13}\exp(\mathrm{i}\Phi),$$

where $\Phi = \phi_3 + \phi_4 - \phi_1$ is the relative phase of the applied fields. From Equation (6), it is clear that, due to the existence of the microwave field, the system becomes sensitive to the relative phase Φ.

In the following, the numerical calculation is used under the case that the microwave-induced coherence is included, which is necessary for phase-sensitive property in the scheme in question. Figure 4 depicts the dependences of the refraction–absorption relation on the relative phase Φ for several different values of the probe detuning $\Delta_1 = 0$ and $\pm\Omega_3$ for the Rabi frequency of the resonant microwave field, $\Omega_4 = 0.8$. One can see that for these different detunings, the maximum index of refraction can always correspond to zero absorption at the appropriate values of the relative phase Φ; with different detunings, the high index of refraction without absorption corresponds to different values of Φ. However, these figures are distinct from those shown in Fig. 3. For example, at $\Delta_1 = 0$, the high index of refraction without absorption corresponds to $\Phi = 2k\pi + \pi$ (points A_1, A_2 in Fig. 4a); at $\Delta_1 = \Omega_3$, – to $\Phi = 2k\pi - \pi/2$ (points B_1, B_2 in Fig. 4b); and at $\Delta_1 = -\Omega_3$, – to $\Phi = 2k\pi + \pi/2$ (points C_1, C_2 in Fig. 4c), where $k = 0, \pm1, \pm2, \ldots$. By comparing Fig. 4 with Fig. 3, we can see that, at the same detunings, there is a phase difference $\pi/2$ when the phenomenon of the high refractive index without absorption appears. This is due to the fact that the microwave-induced coherence between levels $|1\rangle$ and $|4\rangle$ is proportional to $\mathrm{i}\Omega_4$, while the spontaneously generated coherence is proportional to $2\sqrt{\gamma_1\gamma_3}$.

Figure 5 shows the dependences of $\mathrm{Re}\rho_{21}$ and $\mathrm{Im}\rho_{21}$ on the probe detuning Δ_1 at several different (as in Fig. 2) values of the relative phase. The behaviour of the refraction–absorption properties are very similar to the situation shown in Fig. 2 except the phase difference $\pi/2$. From Figs 5a–c, we can also find that the high index of refraction always correspond to zero absorption. For different Φ, the high index of refraction without absorption corresponds to different detunings: when $\Phi = \pi$ (Fig. 5a), it appears at $\Delta_1 = 0$, and when $\Phi = -\pi/2$ (Fig. 5b), it arises at $\Delta_1 = \Omega_3$, which corresponds to the first eigenvalue of the two dressed states. When $\Phi = \pi/2$, [see Figure 5(c)], the high index of refraction without absorption emerges at $\Delta_1 = -\Omega_3$, which corresponds to the second eigenvalue of the two dressed states.

4. Analytical explanation

From all above discussions, we can conclude that a high index of refraction without absorption can be always achieved by choosing proper values of the relative phase, no matter the quantum coherence between the two lower levels is induced by the spontaneous decay or by the microwave field. This interesting phenomenon originates from Eqns (3) and (6),

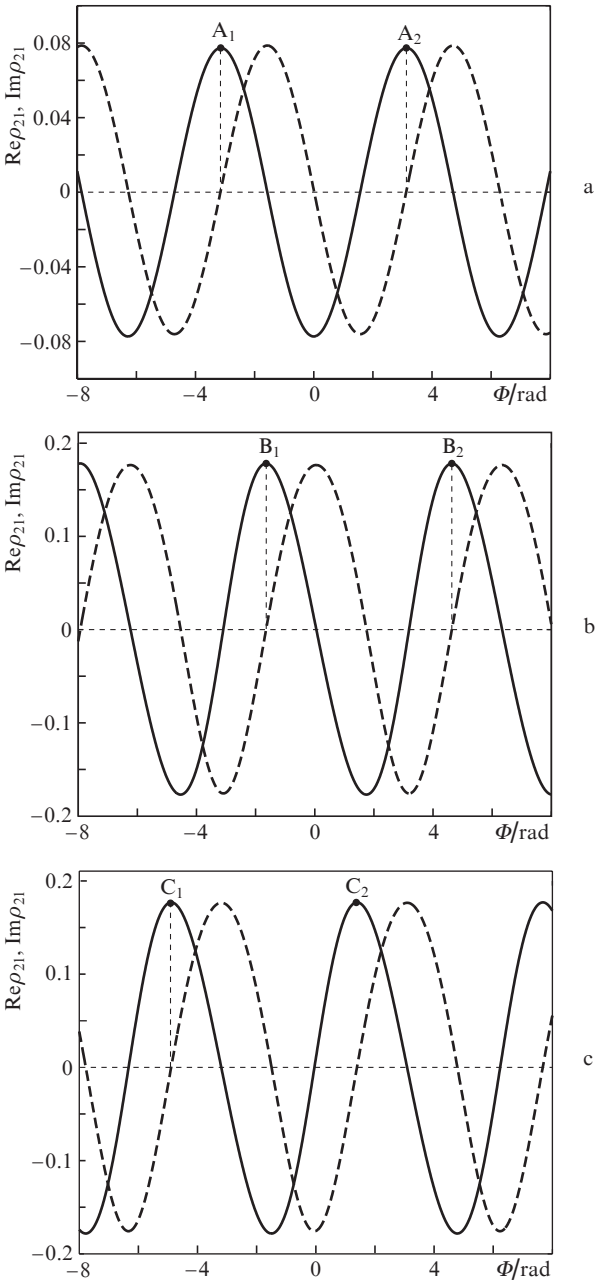

Figure 4. Reρ_{21} (solid curves) and Imρ_{21} (dashed curves) vs. relative phase Φ at probe detuning Δ_1 = (a) 0, (b) Ω_3 and (c) $-\Omega_3$ ($\gamma_1 = \gamma_2 = \gamma_3 = 1$, $\Omega_1 = 0.1$, $\Omega_2 = 0.5$, $\Omega_3 = 10$, $\Delta_2 = -\Delta_1$, $\Delta_3 = 0$, $\Omega_4 = 0.8$).

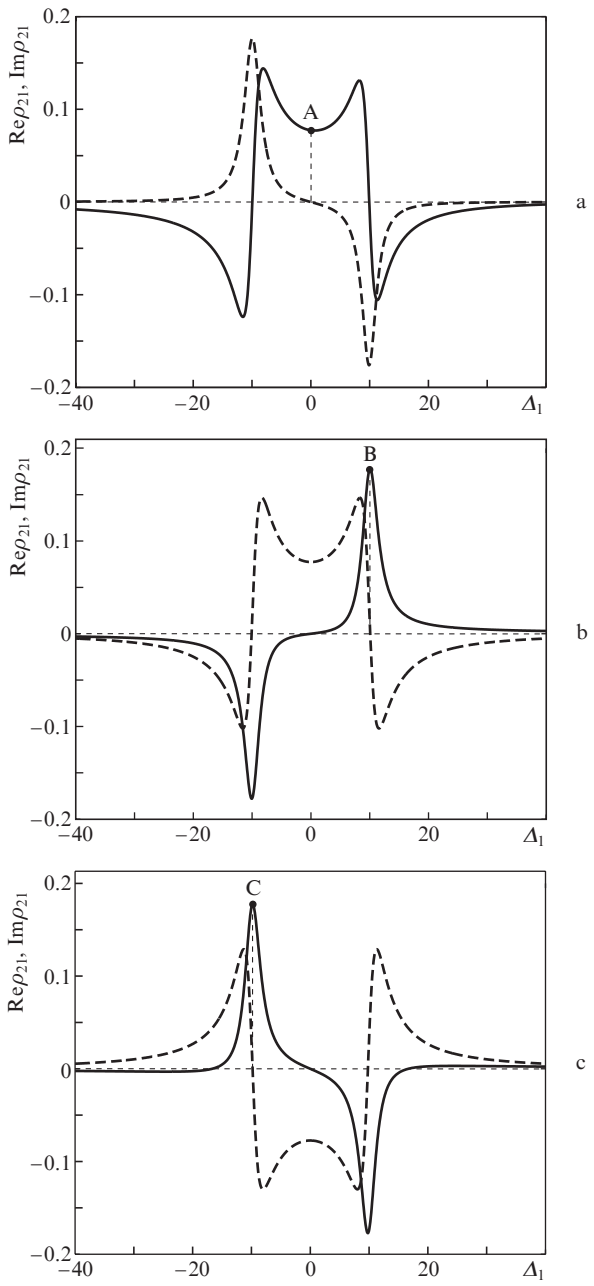

Figure 5. Reρ_{21} (solid curves) and Imρ_{21} (dashed curves) vs. probe detuning Δ_1 at Φ = (a) π, (b) $-\pi/2$ and (c) $\pi/2$. Other parameters are the same as those in Fig. 4.

which indicate that polarisation ρ_{21} depends on the relative phase Φ due to the allowance for the quantum coherence. A simple relationship between the real and imaginary parts of ρ_{21} can be analytically derived:

$$\frac{\mathrm{d}}{\mathrm{d}\Phi}\mathrm{Re}\rho_{21} \propto -\mathrm{Im}\rho_{21}. \tag{7}$$

According to Equation (7), when

$$\frac{\mathrm{d}}{\mathrm{d}\Phi}\mathrm{Re}\rho_{21} = 0,$$

i.e., Reρ_{21} is maximal, the value of Imρ_{21} must be zero. In other words, the maximum index of refraction always corresponds to zero absorption, which means that in these two schemes (SGC scheme and microwave-induced coherence scheme), the high index of refraction without absorption can be always achieved by choosing the proper values of the relative phase Φ. However, it should be pointed out that because the magnitude of the microwave field can be controlled and the microwave-induced coherence is beyond the non-orthogonal condition, the latter scheme is physically different from the former SGC scheme and is practically significant for the control of atom–field systems.

5. Conclusions

In this paper, we have discussed two ways of the control over the refraction–absorption properties of a four-level inverted-

Y system. The first one is implemented by using the spontaneously generated coherence, and the second one is achieved by applying an additional microwave field. Due to the existence of the quantum coherence effect, the refraction–absorption properties are dependent on the relative phase of the applied fields in both driven ways. Therefore, the behaviour of the refractive index can be modified by controlling the relative phase of the applied fields. It has also been found that, with the proper values of the relative phase, the systems in question can exhibit the desirable high index of refraction without absorption, which plays an important role for dispersion compensation in optical communication.

Acknowledgements. This work was partly supported by the National Natural Science Foundation of China (Grant No. 10647007), the Scientific Research Fund of Sichuan Provincial Education Department (Grant No. 13ZB0208) and the Key Research Foundation of Yibin (Grant No. 2014SF031).

References

1. Scully M.O. *Phys. Rev. Lett*., **67**, 1855 (1991).
2. Harris S.E., Sokolov A.V. *Phys. Rev. A*, **55**, R4019 (1997).
3. Xiao Z.H., Kim K. *Opt. Commun*., **282**, 2178 (2009).
4. Yavuz D.D. *Phys. Rev. Lett*., **95**, 223601 (2005).
5. Kalachev A., Kocharovskaya O. *Phys. Rev. A*, **83**, 053849 (2011).
6. Fleischhauer M., Keitel C.H., Scully M.O., et al. *Phys. Rev. A*, **46**, 1468 (1992).
7. Loffler M., Nikonov D.E., Kocharovskaya O.A., et al. *Phys. Rev. A*, **56**, 5014 (1997).
8. Menon S., Agarwal G.S. *Phys. Rev. A*, **61**, 013807 (1999).
9. Barantsev K.A., Litvinov A.N., Kazakov G.A., Rozhdestvenskii Yu.V. *Kvantovaya Elektron*., **42**, 612 (2012) [*Quantum Electron*., **42**, 612 (2012)].
10. Budriga O. *Eur. Phys. J. D*, **66**, 137 (2012).
11. Zeng Z.Q., Hou B.P., Liu F.T., Shao J.X. *Chin. Phys. Lett*., **31**, 034201 (2014).
12. Zibrov A.S., Lukin M.D., Hollberg L., et al. *Phys. Rev. Lett*., **76**, 3935 (1996).
13. Walker D.R., Yavuz D.D., Shverdin M.Y., et al. *Opt. Lett*., **27**, 2094 (2002).
14. Sikes D.E., Yavuz D.D. *Opt. Commun*., **283**, 556 (2010).
15. Barantsev K.A., Litvinov A.N. *Zh. Eksp. Teor. Fiz*., **145**, 653 (2014) [*JETP*, **118**, 569 (2014)].
16. Zeng Z.Q., Wang Y.P., Hou B.P. *Eur. Phys. J. D*, **67**, 76 (2013).
17. Zeng Z.Q., Hou B.P., Liu F.T., Gao Z.H. *Opt. Commun*., **315**, 12 (2014).
18. Yan C.H., Wei L.F., Jia W.Z., Shen J.T. *Phys. Rev. A*, **84**, 045801 (2011).
19. Zhu Y., Saldana J., Wen L.L., Wu Y. *J. Opt. Soc. Am. B*, **21**, 806 (2004).
20. Kilin S.Y., Kapale K.T., Scully M.O. *Phys. Rev. Lett*., **100**, 173601 (2008).
21. Yan M., Rickey E.G., Zhu Y. *Phys. Rev. A*, **64**, 043807 (2001).
22. Kou J., Wan R.G., Kuang S.Q., et al. *Opt. Commun*., **284**, 1603 (2011).
23. Ahmed E., Hansson A., Qi P., et al. *J. Chem. Phys*., **124**, 084308 (2006).
24. Mohapatra A.K., Jackson T.R., Adams C.S. *Phys. Rev. Lett*., **98**, 113003 (2007).
25. Tian S.C., Kang Z.H., Wang C.L., et al. *Opt. Commun*., **285**, 294 (2012).
26. Joshi A., Xiao M. *Phys. Lett. A*, **317**, 370 (2003).
27. Qi J. *Phys. Scr*., **81**, 015402 (2010).
28. Li A.J., Gao J.Y., Wu J.H., et al. *J. Phys. B*, **38**, 3815 (2005).
29. Joshi A., Xiao M. *Phys. Rev. A*, **72**, 062319 (2005).
30. Yang X.H., Zhu S.Y. *Phys. Rev. A*, **78**, 023818 (2008).